Cover Page

Universiteit Leiden

The handle http://hdl.handle.net/1887/38651 holds various files of this Leiden University dissertation

Author: Lucassen, Eliane Alinda
Title: Circadian timekeeping: from basic clock function to implications for health
Issue Date: 2016-03-31

CHAPTER 4

Role of vasoactive intestinal peptide in seasonal encoding by the suprachiasmatic nucleus clock

Eliane A. Lucassen,[1] Hester C. van Diepen,[1] Thijs Houben,[1] Stephan Michel,[1]
Christopher S. Colwell[1,2],*and Johanna H. Meijer[1]*
*C.S.C. and J.H.M. contributed equally to this work.

Eur J Neurosci 2012, 35: 1466-74.

1. Laboratory of Neurophysiology, Department of Molecular Cell Biology,
Leiden University Medical Center, Leiden, the Netherlands.
2. Laboratory of Circadian and Sleep Medicine, Department of Psychiatry and Biobehavioral Sciences,
University of California, Los Angeles, United States.

Abstract

The neuropeptide vasoactive intestinal peptide (VIP) is critical for the proper functioning of the neural circuit that generates circadian rhythms. Mice lacking VIP show profound deficits in the ability to generate many behavioral and physiological rhythms. To explore how the loss of VIP impacts on the intact circadian system, we carried out *in vivo* multiunit neural activity (MUA) recordings from the suprachiasmatic nucleus of freely moving VIP knockout (KO) mice. The MUA rhythms were largely unaltered in the VIP KO mice, with no significant differences being seen in the amplitude or phase of the rhythms in light–dark conditions. Robust differences between the genotypes were revealed when the mice were transferred from light–dark to constant darkness conditions. In addition, the ability of the VIP KO mice to encode changes in photoperiod was examined. Strikingly, the behavioral and physiological rhythms of VIP KO mice showed no adaptation to short or long photoperiods. The data indicate that the intact circadian system can compensate for some of the consequences of the loss of VIP, whereas this peptide is indispensable for endogenous encoding of seasonal information.

Introduction

Circadian rhythms are present in almost all organisms, and have evolved as an adaptation to the rotation of the earth around its axis. In mammals, these rhythms are generated in the suprachiasmatic nucleus (SCN) of the hypothalamus. The SCN consists of approximately 20,000 neurons that produce an endogenous circadian rhythm in multiunit neuronal activity (MUA), reaching its peak during the day and its trough at night.

In order to function adaptively, the SCN neural activity rhythms need to be synchronized to the environment, and a variety of evidence indicates that the light–dark (LD) cycle is the main environmental signal responsible. In addition to its role in the generation of daily rhythms, the SCN is critical for the body's response to seasonal changes. In particular, the neural activity patterns in the SCN change as a function of day-length.[1-4] These photoperiod-induced changes in the patterns of SCN neural activity are thought to underlie seasonal changes in mammals' physiology and behavioral activity patterns.[4-6] Thus, the SCN is critically involved in both circadian and seasonal changes in physiology and behavior. In order to generate a coherent output signal, it is important for individual neurons within the SCN to be mutually synchronized. A major candidate implicated in interneuronal SCN synchronization is vasoactive intestinal peptide (VIP). Anatomically, VIP is expressed in neurons in the ventral, core SCN region that receive light input through the retinohypothalamic tract (RHT). These VIP-expressing cells send projections to the dorsal, shell SCN, as well as leaving the SCN and innervating SCN targets such as the subparaventricular zone.[7-9] Application of VIP alters the firing rate of SCN neurons,[10] induces Per1 expression,[11] and causes phase shifts of the SCN circadian rhythm.[12-14] The loss of VIP or its receptor (VIP receptor 2, VIPR2) disrupts neural activity rhythms of the SCN measured *in vitro*,[15-16] at least partly because of loss of synchrony of the SCN cell population.[17-18] Behaviorally, all VIP-deficient and VIP2R-deficient mice exhibit disruptions in their ability to express a coherent circadian rhythm in constant darkness (DD) as well as alterations in their ability to synchronize to the LD cycle.[17-20]

Synchronization of neurons within the SCN is also important for seasonal encoding mechanisms of the SCN.[1,3,4] In short days, the SCN ensemble rhythm is compressed and shows a narrow peak, whereas in long days, it is decompressed and shows a broad peak. The changes in the waveform pattern of the electrical SCN rhythm arise from changes in phase relationships among activity patterns of single neurons. In short days, subpopulations of SCN neurons are synchronized, whereas in long days, these subpopulations show a broader distribution.[1] An important attribute of the seasonal encoding system is its 'memory' for photoperiod. Even when animals are transferred from the photoperiod into DD, the phase relationships are preserved, and animals continue to show the characteristic behavioral patterns for days–weeks. It is not yet understood how the seasonal information is stored within the SCN, and an immediate question is which transmitter system is involved in this process.

In the present study, we first carried out *in vivo* MUA recordings from the SCN of freely moving VIP knockout (KO) mice and littermate wild-type (WT) controls. We then exposed the VIP KO mice to long (LD16:8) and short (LD8:16) photoperiods and measured the behavioral and physiological responses.

Materials and methods

Animals and housing

The VIP/PHI$^{-/-}$ mouse model was originally generated in the Department of Psychiatry and Biobehavioral Sciences at the University of California in Los Angeles. Mouse genotype was confirmed with a triple-primer PCR assay (see Colwell et al., 2003 for more information). Littermate VIP$^{+/+}$ mice were used as WT control animals in this experiment. The Animal Experiments Ethical Committee of Leiden University Medical Center approved all of the experiments.

Electrode implantation

Male mice were housed under LD12:12, LD18:6 (long day) or LD6:18 (short day) cycles. At a minimum age of 12 wks, the mice were anesthetized with Hypnorm / Dormicum and implanted with tripolar stainless steel electrodes (0.125 mm; Plastics One, Roanake, VA, USA) with a stereotaxic instrument. Two electrodes (polyimideinsulated) were used for differential recordings of the MUA, and one was placed in the gray matter for reference. Aiming for the SCN under a 5° angle in the coronal plane, the following stereotaxic coordinates were used: 0.4 mm anterior of bregma, 0.48 mm lateral to the midline, and 5.44 mm ventral to the surface of the cortex.[21] At the end of the experiment, the position of the electrode was histologically confirmed by passing a small electric current through the electrode, enabling the resulting iron deposition from the tip to be stained with potassium ferrocyanide.

In vivo MUA recordings

All mice had a recovery period after surgery of at least 1 week before placement in the recording cage with a Plexiglas front, and were connected to the recording system with a counterbalanced swivel system that allowed the mice to move freely. After appropriate amplification and filtering (0.5–5 kHz) of the signal, the action potentials were detected with window discriminators and counted in 10-s epochs. MUA data were smoothed with a penalized least-squares algorithm[22] to describe the waveform of the rhythm, and to determine peak and trough time, and peak width. Behavioral activity was measured simultaneously with passive infrared sensors. Mice were initially held for 5 days under an LD12:12 cycle followed by DD. The peak width was determined per mouse in the smoothed curve at half-maximum values and averaged.

The time of the peak and trough were determined with zeitgeber time (ZT) 12 defined as lights-off. The MUA data were smoothed, and the mean period of MUA was calculated by determining peak-to-peak time in DD per mouse. The mean amplitude was calculated per cycle, per mouse, by subtraction of trough height from peak height. The mean amplitude decrease after transfer to DD was calculated by dividing the mean amplitude levels in DD by the mean amplitude levels in the LD cycle. Phase advances in MUA were calculated by comparing the time of the 50% level of the final downward slope in the LD cycle and the half-maximum level of the first downward slope in DD, and were corrected for endogenous period.

Mice were entrained to short and long photoperiods for 25 days before recordings, as shorter entrainment periods did not lead to consistent waveform changes in the MUA rhythm in WT mice.[1] Mice exposed to long and short days were recorded for at least 5 days in the LD cycle and for approximately 5 days in DD. The peak width and phase of MUA were calculated. For mice that were exposed to long photoperiods, the quality of the rhythm decreased, and not all peaks could be used for the analysis. We only used peaks that had an amplitude of at least 30% of the amplitude in the LD cycle.

Behavioral data collection and analysis

We used passive infrared sensors to register behavioral activity during the MUA recording (**Fig. 1, Fig. 2, Fig. 4, Suppl. Fig. 2**). We made activity profiles by adding behavioral activity in 10-min bins per 24 hrs, and we made MUA profiles by adding smoothed MUA data per 24 hrs (**Suppl. Fig. 2**). For all other behavioral analyses, behavioral activity was monitored by the wheel-running activity of individually housed mice, recorded in 1-min bins (Clocklab; Actimetrics, Wilmette, IL, USA). VIP KO mice and their WT littermates were recorded for 30 days in either short or long days, and the recordings were continued for at least 14 days after release into DD. The duration of the active phase of the activity rhythm (alpha) was determined manually in individual mice by estimation of the activity onsets and offsets on each day. Amplitudes of behavioral rhythms were determined in individual mice by F periodogram analysis over the first 10 days of wheel running activity in DD. The phase advance in behavioral activity after release into DD was determined by fitting a straight line through all activity onsets, and was corrected for endogenous period.

Statistical analysis

Independent samples two-sided *t*-tests were performed in SPSS, and differences were considered to be significant if $P < 0.05$. To assess the normality of the data obtained from the *in vivo* MUA recordings, Shapiro–Wilk tests were performed. All data were normally distributed, except for the phase advance after lights off in WT mice ($P = 0.01$), so we performed a Mann–Whitney test. All values are shown as mean ± standard error of the mean. For analysis of

behavioral activity patterns, calculations of differences in alpha, in total behavioral activity and in amplitude, we used independent samples two-sided *t*-tests.

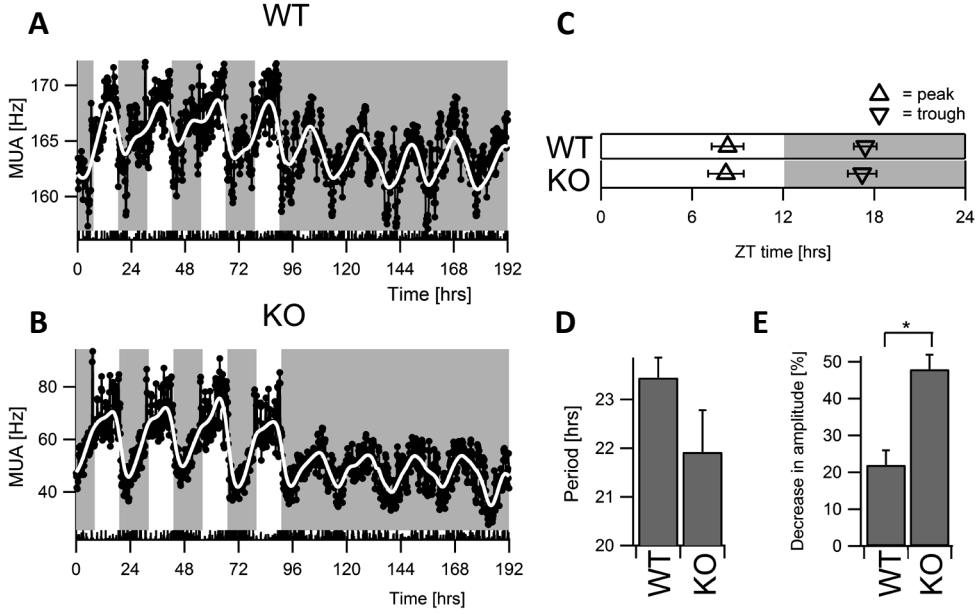

Fig. 1. SCN MUA rhythms recorded from the SCN of freely moving mice. Representative examples of MUA rhythms recorded from the SCN of a WT mouse (**A**) and a VIP KO (**B**) mouse. The mice were initially held in an LD12:12 cycle, and subsequently placed into DD. Individual data points represent 10-min epochs. Smoothed data are indicated by a white line. For this and subsequent figures, a white background indicates light exposure, and a gray background represents darkness. Behavioral activity was measured with a passive infrared sensor, and is depicted at the bottom of each plot. (**C**) The mean peak (upward triangles) and trough (downward triangles) in the MUA rhythms recorded when mice were held in LD12:12. Symbols show means ± standard errors of the mean in this and subsequent figures. (**D**) Mean period of MUA in DD in WT and VIP KO mice. (**E**) The mean (%) decrease in amplitude of the MUA level when mice were switched from LD12:12 to DD as a percentage of baseline MUA levels in each genotype. The asterisk indicates a significant difference at $P < 0.01$ measured with *t*-tests.

Results

Behavioral rhythms

Wheel-running activity was measured under LD12:12 and DD conditions to confirm the VIP-deficient phenotype observed in previous studies (see **Suppl. Fig. 1** for examples). All of the VIP KO (n = 8) and WT littermate (n = 7) mice showed clear rhythms of locomotor activity in LD conditions. When transferred to DD, VIP KO mice, in contrast to WT mice, began behavioral activity 5.59 ± 0.78 hrs earlier than what would be expected on the basis of their previous activity rhythm under LD conditions. All VIP KO mice remained rhythmic during the first 10 days in DD, as measured by F periodogram analysis. Their free-running period was

shorter (23.31 ± 0.38 hrs) than that of WT mice (23.73 ± 0.06 hrs), but this difference was not significant (*P* = 0.33).

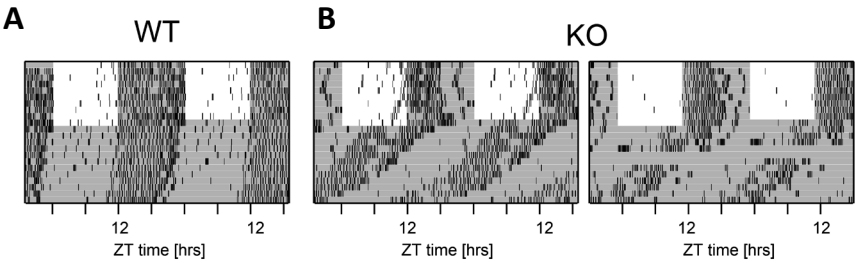

Suppl. Fig. 1. Behavior of WT and VIP KO mice in LD12:12 and in DD. Behavior WT and VIP-deficient mice in LD12:12 and in DD. Typical examples of wheel running activity of a WT (**A**) and two VIP KO mice (**B**) in LD12:12 and consecutive release in continuous dark. Each horizontal row shows behavior over a 24 hr cycle with a white background representing light. Successive days are plotted from top to bottom.

MUA rhythms

Long-term MUA rhythms were recorded from the SCN of VIP KO (*n* = 5) and WT littermate (*n* = 6) mice (**Fig. 1A and B**). Recordings were performed for five cycles in LD12:12, and then for five cycles in DD. All of the VIP KO and WT mice showed diurnal rhythms in MUA when exposed to the LD cycle, with a peak in MUA in the middle of the day, and a trough in the middle of the night. The mean times to peak after lights-on (ZT 0) were 8.34 ± 1.05 hrs in WT mice and 8.22 ± 1.17 hrs in VIP KO mice (*P* = 0.94, *t*-test). MUA reached its trough at ZT 17.42 ± 0.76 hrs and ZT 17.21 ± 0.94 hrs in WT and VIP KO mice, respectively (*P* = 0.79, *t*-test). Under these conditions, the durations of the width of the peak in MUA measured at half maximum levels were 11.81 ± 0.32 hrs in WT mice and 12.17 ± 0.41 hrs in VIP KO mice (*P* = 0.50, *t*-test). Thus, in LD conditions, VIP KO mice were able to maintain a robust rhythm in electrical activity with characteristics and phasing comparable to WT rhythms.

All of the VIP KO (*n* = 5) and WT (*n* = 6) mice showed circadian rhythms in MUA when the mice were held in DD. In DD, VIP KO mice tended to have a shorter free-running period of the MUA rhythm (VIP KO, 21.92 ± 0.86 hrs; WT, 23.45 ± 0.41 hrs), but this difference was not significant (*P* = 0.16, *t*-test). The mean free-running periods of MUA rhythms were similar to the periods in wheel-running activity in VIP KO mice (*P* = 0.11) and in WT mice (*P* = 0.55). The width of the peak in MUA was almost identical between WT mice (11.14 ± 0.34 hrs) and VIP KO mice (11.31 ± 0.41 hrs; *P* = 0.76). There were two robust differences between the genotypes when they were transferred from LD conditions to DD. First, the amplitude of the MUA rhythm decreased more in VIP KO mice (48% ± 8%) than in WT mice (22 ± 4%, *P* < 0.01, *t*-test). Second, the MUA activity rhythm was dramatically phase advanced (**Fig. 2B**). The half-maximum level of the downward slope in MUA, which is strongly correlated with activity onset, started 5.68 ± 1.42 hrs before project lights-off in VIP KO mice and at 0.19 ± 0.58 hrs in

WT mice ($P < 0.01$, Mann–Whitney test). The start of behavioral activity of the same VIP KO mice was earlier than expected on the basis of endogenous period when lights were switched off (**Fig. 2A**). Average waveforms in MUA under LD conditions did not differ between the groups (**Fig. 2C**). We observed that the downward slope of MUA was strongly correlated with activity onset in both strains of mice (**Fig. 2D**). We made activity profiles of total behavioral activity per 24 hrs and 24 hrs. profiles of concurrently measured MUA of both genotypes (**Suppl. Fig. 2**). We calculated the level of MUA at which half of the total behavioral activity had occurred. On average, this occurred at the same level of MUA in WT mice (1 ± 0%) and in VIP KO mice (7 ± 4%, $P = 0.28$, *t*-test).

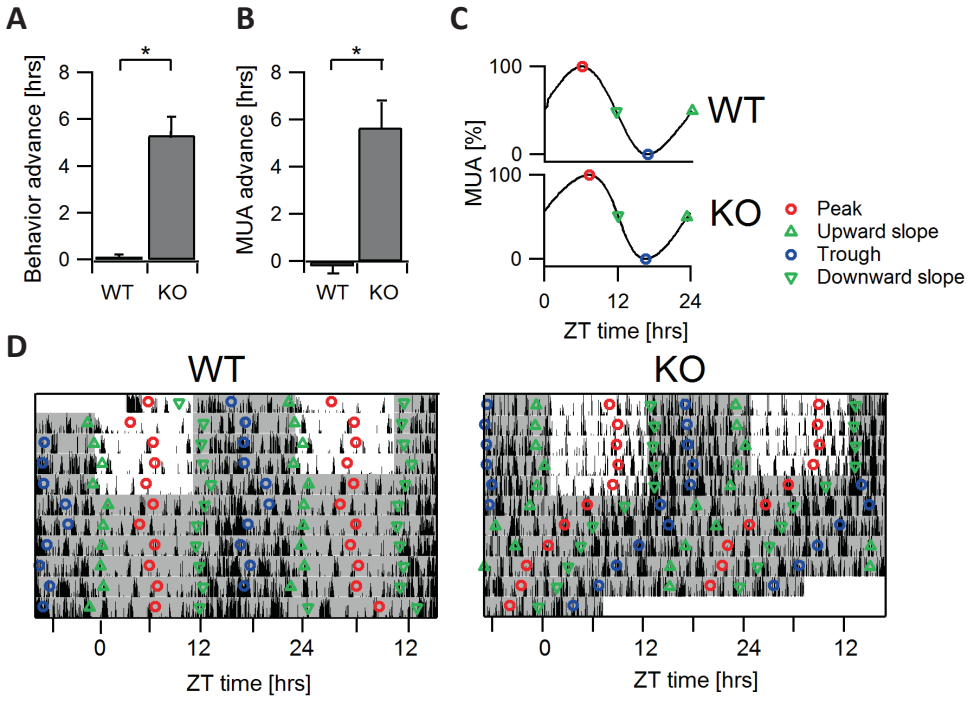

Fig. 2. Phase advance in behavior and MUA after release in DD. Bar graphs compare the phase advance in behavior (**A**) and MUA (**B**) when a mouse was released into DD from the LD cycle. The asterisk indicates a significant difference at $P < 0.01$ measured with *t*-tests (**A**) or Mann–Whitney tests (**B**). (**C**) The average waveforms of MUA in WT and VIP KO mice in LD12:12, made by adding smoothed MUA activity waveforms of all mice used for analysis. Peaks and troughs in MUA are displayed as red and blue circles, respectively. Half-maximum values of MUA are indicated by green triangles. (**D**) Representative example of behavioral activity of WT (left panel) and VIP KO (right panel) mice measured with a passive infrared sensor. Each horizontal row represents a double-plotted 24 hrs. day, with successive days plotted from top to bottom. Reference points (see legend) from the recorded MUA rhythm are superimposed on the locomotor activity plot.

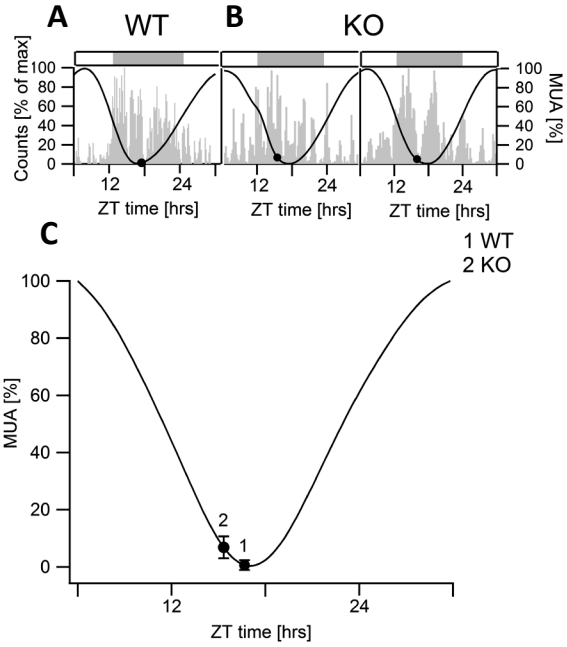

Suppl. Fig. 2. Correlation between behavior and MUA in WT and VIP KO mice in LD12:12. Correlation between behavior and MUA in WT and VIP-deficient mice in LD12:12. Typical examples of activity profiles of a WT mouse (**A**) and of two VIP KO mice (**B**). Behavioral activity as measured by passive infrared sensors is depicted in grey in 10-minute bins as a percentage of maximal activity per bin size. The black curve shows normalized mean multiunit electrical activity (MUA). Light is depicted at the top of the plot with grey indicating darkness. The point in time and relative to MUA value where 50% of total behavioral activity had occurred is indicated as black dots. (**C**) Mean normalized MUA values of WT and VIPdeficient mice are indicated by the black line. The mean point in time where 50% of total behavioral activity had is depicted by black dots for WT (1) and VIP KO (2) mice and were not significantly different (*t*-test, $P = 0.28$).

Behavioral and MUA rhythms measured in long and short photoperiods

The wheel-running activity of VIP KO and WT mice was measured in short (LD8:16; KO, $n = 16$; WT, $n = 17$) and long (LD16:8; KO, $n = 11$; WT, $n = 16$) photoperiods, respectively. Mice were held in the LD cycle for 30 days, and were then released into DD (**Fig. 3; Table 1**). All of the mice showed a robust daily rhythm in LD conditions, with activity increasing sharply after lights-off. The amplitude of the daily rhythm in locomotor activity was reduced ($P < 0.01$) in VIP KO mice as compared with WT controls, with the mutant mice in the long days exhibiting the lowest amplitude (**Table 1**). Total behavioral activity was significantly lower in the VIP KO mice ($P < 0.01$) than in controls, but did not differ between long and short photoperiod exposure in either genotype. Following entrainment to long days and release into DD, VIP KO mice showed a phase advance of behavioral activity of 12.74 ± 0.61 hrs as compared with the time of expected behavioral onset based on endogenous period. After short day exposure and release into DD, VIP KO mice started activity 3.85 ± 0.28 hrs earlier than expected. The behavioral phase advance in DD was significantly ($P < 0.05$) altered by exposure to the different photoperiods (**Fig. 3**). In DD, VIP KO mice showed lower amplitude rhythms than WT controls (**Table 1**).

Table 1. Behavioral parameters of mice in short (LD8:16) and long (LD16:8) photoperiods.

	Short day		Long day	
	VIP KO	**WT**	**VIP KO**	**WT**
Alpha in LD (hrs)*,†	12.8 ± 0.3	12.9 ± 0.3	6.4 ± 0.2	7.7 ± 0.1
Alpha in DD (hrs)*,‡,§	9.3 ± 0.5	12.6 ± 0.3	11.2 ± 0.6	9.0 ± 0.3
Period in DD (hrs)	23.9 ± 0.2	23.8 ± 0.2	23.8 ± 0.4	23.9 ± 0.2
Amplitude in DD (hrs)†,‡,§	0.6 ±0.1	0.9 ± 0.0	0.4 ± 0.2	0.9 ± 0.0
Phase advance (hrs)†,‡,§	3.9 ± 0.3	0.2 ± 0.1	12.7 ± 0.6	0.0 ± 0.1

*$P < 0.05$ between short and long days in WT mice; †$P < 0.05$ between short and long days in VIP KO mice; ‡$P < 0.05$ between genotypes in short days; §$P < 0.05$ between genotypes in long days.

One of the important changes in circadian behavior observed in mice held in different photoperiods is an adaptive alteration in the duration of the night activity interval (alpha) (**Fig. 3**). WT mice showed a significantly ($P < 0.05$) longer alpha when held in short days (12.9 ± 0.3 hrs) than when held in long days (7.7 ± 0.0 hrs). Similar differences in alpha ($P < 0.05$) were observed in VIP KO mice held in short days (12.8 ± 0.3 hrs) or long days (6.4 ± 0.2 hrs). As expected, when WT animals were released into DD, alpha remained significantly ($P < 0.05$) longer after short days (12.6 ± 0.3 hrs) than after long days (9.0 ± 0.3 hrs). This history-dependent change in alpha (after-effects) was lost in the mutant mice. When VIP KO mice held in short days were released into DD, the alpha of the activity rhythm was only 9.3 ± 0.5 hrs, and those that were in long days showed an alpha of 11.4 ± 0.5 hrs.

Finally, long-term MUA rhythms were recorded from the SCN of VIP KO mice held in long days ($n = 6$) or short days ($n = 6$; **Fig. 4**). Recordings were performed for five cycles in the LD condition, followed by five cycles in DD. All of the VIP KO mice showed diurnal rhythms in MUA, whether exposed to a short or a long photoperiod. The average width of the MUA peak measured at halfmaximum levels was significantly ($P < 0.001$, *t*-test) decreased when the mice were held in short day (9.82 ± 0.38 hrs) as compared with long day (14.40 ± 0.45 hrs) conditions. In three mice, MUA was measured in more than one photoperiod consecutively (**Suppl. Table 1**). The peak width of MUA lengthened with longer photoperiod exposure. When mice were transferred to DD, all of the VIP KO mice (6 / 6) continued to show clear circadian rhythms in MUA after short day exposure. In contrast, after exposure to long photoperiods, some of the VIP KO mice (2 of 6) lost the circadian rhythmicity in MUA, and the remaining mice showed weak rhythms. Therefore, we could only reliably determine period and phase advance in MUA after short day exposure: 22.96 ± 0.13 and 1.97 ± 0.81 hrs. Importantly, after exposure to DD, the prior photoperiod had no significant impact on the MUA peak width (**Fig. 4**). The mean widths of the peak were 10.93 ± 0.83 and 12.16 ± 0.77 hrs after short and long day exposure ($P = 0.37$, *t*-test). Thus, for both the behavioral and MUA rhythms, the VIP KO mice lost the photoperiod-driven plasticity in output.

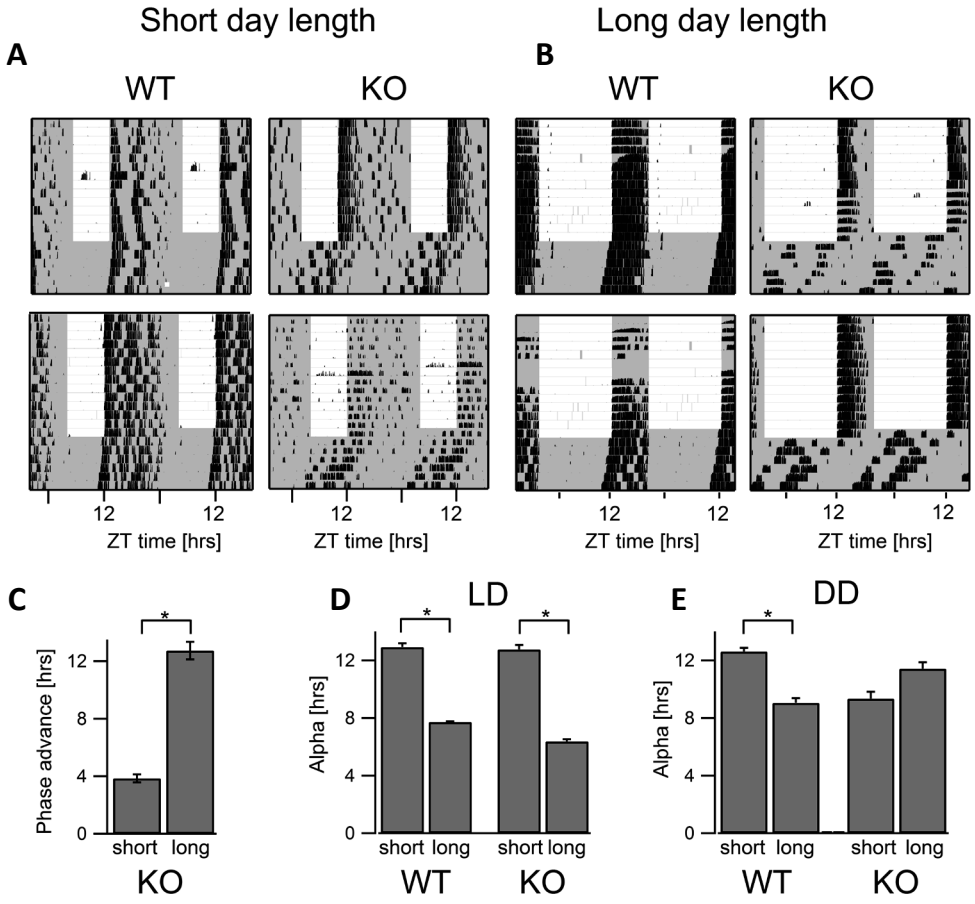

Fig. 3. Behavior of VIP KO mice exposed to short and long photoperiod conditions. Representative wheel-running activity records of WT and VIP KO mice under (**A**) short (LD6:18) and (**B**) long (LD18:6) photoperiod exposure. Each horizontal row represents wheel-running activity over a 24 hr cycle. Successive days are plotted from top to bottom. (**C**) Bar graphs plotting the behavior phase advance measured at the LD ⁄ DD transition for VIP KO mice in each photoperiod. Bar graphs showing the duration of the active phase (alpha) in each genotype under LD (**D**) and DD (**E**) conditions. The asterisk indicates a significant difference at $P < 0.05$ measured with *t*-tests.

Suppl. Table 1. Width of the peaks in MUA in a subpopulation of VIP KO mice that were measured in multiple photoperiods.

	Short day	**LD12:12**	**Long day**
Animal 1	9.04 hrs	-	13.05 hrs
Animal 2	9.54 hrs	11.66 hrs	15.51 hrs
Animal 3	-	13.76 hrs	15.51 hrs

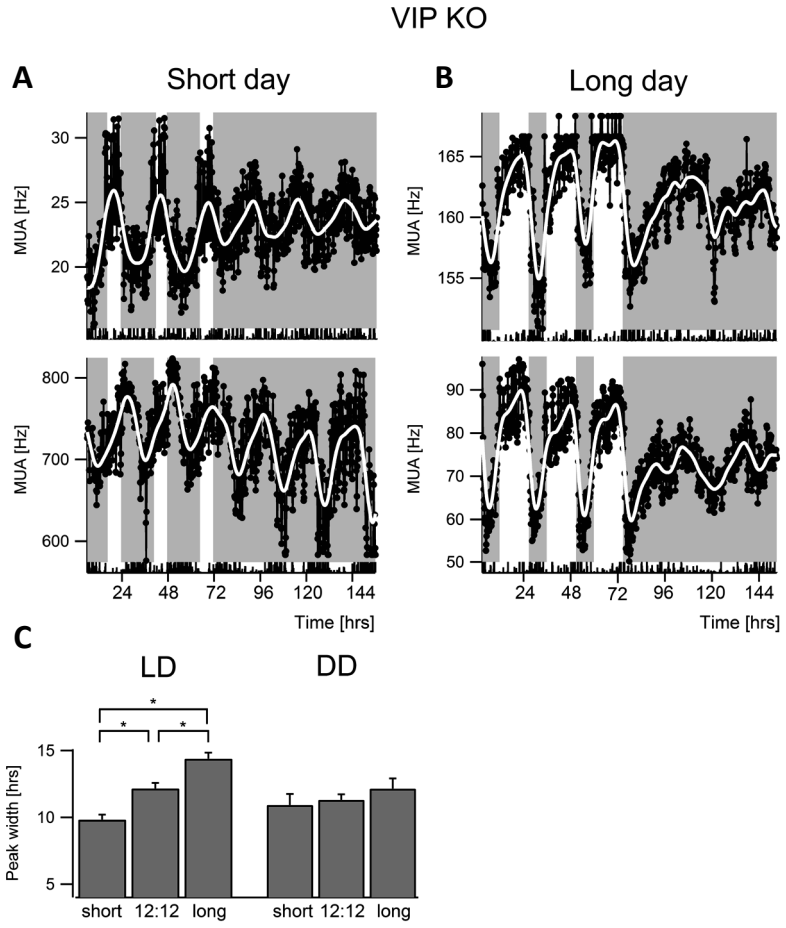

Fig. 4. MUA rhythms recorded from the SCN of VIP KO mice exposed to short and long photoperiods. Representative examples of MUA recordings from the SCN of VIP KO mice in (**A**) short (LD8:16) or (**B**) long (LD16:8) photoperiods and after release into DD. For visibility of the data, the first 3.5 days in DD are shown, but traces are part of a longer recording. Note the loss of circadian rhythmicity in the mice (B, top panel) after they had been released into DD. The white line shows the smoothed data (10-min bins). Behavioral activity as recorded with passive infrared sensors is depicted below. (**C**) The width of the peak that was measured at half-maximum electrical activity levels from each genotype. After exposure to long days, the MUA rhythms were disturbed and not all peaks could be used for the measurements. The asterisk indicates a significant difference at $P < 0.05$ measured with *t*-tests. As MUA rhythms became sloppy after long day exposure, not all peaks could be used for peak width determination.

Discussion

MUA rhythms

We implanted electrodes into the SCN of VIP KO mice and littermate WT controls, and continuously recorded MUA in freely moving mice. Under LD12:12 conditions, VIP KO mice showed strong daily rhythms in MUA that peaked during the second half of the day and reached their trough in the middle of the night (**Fig. 1**). The amplitudes and the phase of

the rhythms could not be distinguished from those recorded from the SCN of WT mice. When VIP KO mice were transferred to DD, the MUA rhythm continued, but displayed a reduction in amplitude that was significantly larger than the amplitude drop observed in WT mice (**Fig. 1**). Also, upon release into DD, the MUA rhythm of VIP KO mice showed a phase advance of about 6 hrs (**Fig. 2**), consistent with behavioral findings in earlier reports.[17,18,20] We analysed the half-maximum levels of the downward slope of MUA, as this phase of the rhythm is closely correlated with behavioral onset.[23] We found that the phase advance of the electrical activity rhythm was similar to the phase advance of the behavioral activity rhythm. We considered whether this shift reflects an unmasking of the rhythm in DD. As the electrical activity rhythm of the SCN peaked at the middle of the day under LD conditions, we have no evidence for masking of the SCN rhythm by the light. Our results indicate that, in both LD and DD conditions, the VIP KO mice show a stable phase relationship between the SCN and behavioral activity, and start their activity at the 50% level of the falling slope, as do WT mice.

The impact of VIP deficiency varies with output

As a result of recent work, it is becoming clear that the impact of the loss of VIP or VIPR2 varies with the output being measured. For example, in DD, the wheel-running activity in VIP KO mice is reduced in amplitude and coherence, and declines into arrhythmicity over the course of several weeks,[20] whereas VIPR2 KO mice are apparently arrhythmic from the start of constant conditions.[18] Rhythms in body temperature,[24-26] feeding and metabolism[27] are phase advanced but remain relatively intact. Rhythms in sleep (non-rapid eye movement and rapid eye movement) show reduced day–night amplitude and a phase advance in LD conditions.[24, 28] Rhythms in heart rate in both VIP and VIPR2 mutants are low-amplitude or arrhythmic in LD and DD conditions.[24,26] Similarly, rhythms in the blood levels of adrenocorticotropic hormone and cortisol are all lost in VIP KO mice in both LD and DD conditions.[29] With the present work, we see for the first time what is occurring at the level of the SCN *in vivo*, and find that the overall SCN neural activity rhythm is normal in LD conditions (**Fig. 1**). This suggests that we may need to look to the output pathways to explain the variability in the impact of the loss of VIP on SCN-driven behaviors. Presumably, the SCN projects to extra-SCN tissues and peripheral outputs via interneurons, particularly those that regulate autonomic outflow from the paraventricular nucleus or the brainstem, and / or those that drive the pituitary output and hence adrenal or other endocrine rhythms.[30] Many of these interneurons are VIPergic, and VIP may therefore be required for communication between the SCN and peripheral tissues to drive rhythms in behavior and other biological processes.[7,31-33]

Cellular consequences

The quality of the rhythm in MUA is remarkable, given the compelling evidence that VIP plays a critical role in coupling cells in the SCN circuit.[34] Within the SCN, genetic loss of VIP or VIPR2 disrupts circadian rhythms in neural activity in the SCN population,[15,16] where the

loss of VIP decreases the number of electrically rhythmic SCN neurons and weakens the synchrony among the rhythmic SCN neurons.[17,18] Even at the molecular level, the temporal expression of Per1, Per2 and Bmal1 is disrupted in the SCN.[35] SCN explants from VIP or VIPR2 KO mice showed low-amplitude rhythms in PER2::LUC and PER1::LUC bioluminescence that were not altered in phase as compared with controls.[35-37] Recent work by Maywood et al.[38] has demonstrated that paracrine signalling is sufficient to induce rhythmicity in VIP-deficient SCN slices, and that VIP plays a predominant role in mediating this coupling as measured by PER2::LUC bioluminescence. All of the analyses of the VIP and VIPR2 KO mice indicate that the coupling within the SCN network is greatly reduced by the loss of VIP / VIPR2 signalling, and that the VIP KO mice can be considered to have a 'broken' SCN network.

System-level compensation

The present results raise the question of what is occurring in the intact system that enables the SCN to maintain strong rhythms in MUA in the presence of reduced cellular synchrony resulting from the loss of VIP. The most obvious explanation is that light directly stimulates SCN activity when animals are kept in an LD cycle.[39,40] The decreased behavioral amplitude in DD is also explainable by an absence of entraining light signals. The melanopsin expressing retinal ganglion cells are both directly light-sensitive and receive information from rods and cones.[41-43] These melanopsin-expressing retinal ganglion cells thus encode ambient lighting[44] and generate action potentials that travel down the RHT and reach the SCN. The RHT terminals release glutamate[8] and, under certain conditions, the neuropeptide pituitary adenylate cyclaseactivating peptide.[45] The net result of RHT stimulation is an increase in the firing rate of SCN neurons. Prior work with VIP KO mice demonstrated that the direct effects of light in suppressing activity and of darkness in enhancing activity are completely unaltered by the loss of VIP.[20] Therefore, in an LD cycle, the direct effects of light and dark on MUA are likely to play a major role in maintaining the rhythmicity in SCN physiology and behavior. Previous work has also provided evidence that SCN neural activity is influenced by activity in other brain regions,[46,47] which may explain why, in VIP KO animals, the rhythms in DD are maintained *in vivo*, whereas the rhythms measured *in vitro* are severely decreased.[16,17] Prior studies with the VIPR2 KO mice have also found behavioral[48] and physiological[24] evidence that activity is a strong regulator of rhythmicity in these mice. A variety of earlier studies have noted that locomotor activity itself can modify SCN activity.[49-52] The direct regulation of SCN firing by lighting and activity levels would not be detected in the *in vitro* recording, and could be viewed as a systems-level compensation for the loss of coupling in the VIP KO mice.

Role of VIP in seasonal encoding

The SCN serves as a seasonal clock through its ability to encode daylength.[4,53,54] In line with previous literature,[1,55] the duration of behavioral activity (alpha) was broadened or

compressed when WT mice were exposed to short and long days, respectively (**Fig. 3**). Interestingly, alpha in VIP KO mice was shorter under long than under short photoperiods. When mice were transferred to DD, alpha remained highly correlated with the previous length of photoperiod in WT mice. In VIP KO mice, however, the duration of alpha was not shorter after long day exposure following release into darkness. In fact, alpha was even longer after long days, and we cannot explain this phenomenon. We therefore conclude that seasonal encoding is greatly compromised in VIP KO mice. Similar to observations in LD12:12 conditions, VIP KO mice exposed to different photoperiods showed a rapid and large phase advance with the transition to DD, but the amplitude of the phase advance was dependent on the previous photoperiods (**Fig. 3**). The phase advance was particularly large after exposure to long photoperiods, and was much smaller, and almost the same as, the behavior of WT mice following exposure to short photoperiods. The fact that the behavior of mice after short days resembled the behavior of WT mice may indicate that the short photoperiod has acted as a strong synchronizer, thereby normalizing the behavior of VIP KO mice.

To test whether the impairment in seasonal encoding in VIP KO mice is based on deficiencies within the SCN clock, we investigated the impact of photoperiod on SCN MUA waveform (**Fig. 4**). The waveform of the SCN rhythm shows major differences in response to long and short photoperiods that are brought about by changes in synchrony among molecular and electrical activity rhythms of SCN neurons.[1,3,56-59] A major question that follows from these results concerns the underlying mechanism of phase synchrony *vs.* desynchrony in seasonality. To investigate the putative role of VIP, we measured the electrical activity patterns from SCN neurons in VIP KO mice exposed to short and long days (**Fig. 4**). VIP KO mice showed a broadening of their MUA patterns when they were kept in long days, and a lengthening when kept in short days. The broadness of the peaks at half-maximum levels differed significantly between the photoperiods (14.6 *vs.* 9.8 hrs), which is similar to what is seen in WT animals.[1] Importantly, the MUA of three mice was recorded in multiple photoperiods. The results from these three recordings showed the same photoperiod-driven changes in peak width that we observed in the population (**Suppl. Table 1**). Interestingly, when VIP KO mice were transferred to DD, the width of the MUA profiles was indistinguishable between the groups from long and short photoperiods. It is well accepted that the 'after-effects' in DD indicate the storage of photoperiodic information in the SCN clock. In other words, to test the encoding capacity of the SCN for photoperiod information, the waveform of the rhythm should be evaluated after termination of the light cycle. In our results, the peak width in long days did not exceed the peak width in short days, and in fact it became narrower. The absence of any after-effect on the electrical activity rhythm therefore suggests a total absence of seasonal encoding capability of the SCN in the absence in VIP.

Although photoperiod did not affect the width of the peak, it did affect the phase advancing response of the MUA rhythm when the mice were transferred to DD (**Fig. 3E**). The

phase advance was about 10 hrs after exposure to long days and about 2.5 hrs after exposure to short days. These findings were consistent with the magnitude of the behavioral advances that we observed in VIP KO mice. Finally, we note that the overall quality of the rhythm in both behavior and in MUA activity, as indicated by the amplitude, was better after exposure to short photoperiods than after exposure to long photoperiods. Possibly, the short days functioned as a strong synchronizer, resulting in an absence of a strong phase advancing response and a diminished attenuation of the rhythm in darkness.

Conclusion

The robustness of the rhythm in electrical impulse frequency of the SCN *in vivo*, as compared with previous *in vitro* recordings,[16,17] indicate that communication between neuronal networks can compensate for the absence of VIP-induced synchrony among SCN neurons. The SCN MUA is acutely increased by retinal input,[40] and we speculate that the direct effect of light boosts the magnitude of the MUA rhythms. Possibly, light input maintains phase coherence via the RHT or through behavioral feedback effects, via the geniculohypothalamic input or the median raphe. Additional regulatory effects of behavioral activity and sleep from other brain regions on SCN activity are also likely, [46,49,50] and need to be further explored. Prior work has provided elegant evidence that SCN intercellular coupling provides robustness in the circadian system against genetic perturbations.[60] Here, we show that the intact SCN circuit can overcome the dysfunction caused by the loss of intercellular coupling in the SCN. To put it another way, as important as VIP is for the coupling of SCN neurons, the intact system appears to be able to compensate for its loss, at least under some lighting conditions. However, our findings also indicate that there are some functions that require VIP-mediated intercellular coupling, for example the reorganization of the SCN circuit that is part of the adaptation to changes in photoperiod. Without VIP, both the behavior and the physiology of the SCN appear to be unable to adapt to seasonal changes, and the 'memory' for photoperiod is lost. This is an important finding in the search for mechanisms underlying the consolidation of phase synchrony within the SCN.

Acknowledgements

We thank Hans Duindam, Jan Janse and Sander van Berloo for excellent technical support. The work was supported by a grant to J. H. Meijer from the EC FP6 integrated project 'EUCLOCK' (contract number 018741), by the TOPGO.L.10.035 grant from NWO (number 91210064), and by CHDI Foundation grant A-2702 to C. S. Colwell.

References

1. VanderLeest HT, Houben T, Michel S, et al. (2007) Seasonal encoding by the circadian pacemaker of the SCN. *Curr Biol* 17:468–473.
2. VanderLeest HT, Rohling JH, Michel S, Meijer JH (2009) Phase shifting capacity of the circadian pacemaker determined by the SCN neuronal network organization. *PLoS ONE* 4:e4976.
3. Brown TM, Piggins HD (2009) Spatiotemporal heterogeneity in the electrical activity of suprachiasmatic nuclei neurons and their response to photoperiod. *J Biol Rhythms* 24:44–54.
4. Meijer JH, Michel S, Vanderleest HT, Rohling JH (2010) Daily and seasonal adaptation of the circadian clock requires plasticity of the SCN neuronal network. *Eur J Neurosci* 2:2143–2151.
5. Goldman BD (2001) Mammalian photoperiodic system: formal properties and neuroendocrine mechanisms of photoperiodic time measurement. *J Biol Rhythms* 16:283–301.
6. Ebling FJ, Barrett P (2008) The regulation of seasonal changes in food intake and body weight. *J Neuroendocrinol* 20:827–833.
7. Abrahamson EE, Moore RY (2001) Suprachiasmatic nucleus in the mouse: retinal innervation, intrinsic organization and efferent projections. *Brain Res* 916:172–191.
8. Antle MC, Smith VM, Sterniczuk R, Yamakawa GR, Rakai BD (2009) Physiological responses of the circadian clock to acute light exposure at night. *Rev Endocr Metab Disord* 10:279–291.
10. Reed HE, Cutler DJ, Brown TM, et al. (2002) Effects of vasoactive intestinal polypeptide on neurones of the rat suprachiasmatic nuclei *in vitro*. *J Neuroendocrinol* 14:639–646.
9. Golombek DA, Rosenstein RE (2010) Physiology of circadian entrainment. *Physiol Rev* 90:1063–1102.
11. Nielsen HS, Hannibal J, Fahrenkrug J (2002) Vasoactive intestinal polypeptide induces per1 and per2 gene expression in the rat suprachiasmatic nucleus late at night. *Eur J Neurosci* 15:570–574.
12. Reed HE, Meyer-Spasche A, Cutler DJ, Coen CW, Piggins HD (2001) Vasoactive intestinal polypeptide (VIP) phase-shifts the rat suprachiasmatic nucleus clock *in vitro*. *Eur J Neurosci* 13:839–843.
13. Meyer-Spasche A, Piggins HD (2004) Vasoactive intestinal polypeptide phase-advances the rat suprachiasmatic nuclei circadian pacemaker *in vitro* via protein kinase A and mitogen-activated protein kinase. *Neurosci Lett* 358:91–94.
14. An S, Irwin RP, Allen CN, Tsai C, Herzog ED (2011) Vasoactive intestinal polypeptide requires parallel changes in adenylate cyclase and phospholipase C to entrain circadian rhythms to a predictable phase. *J Neurophysiol* 105:2289–2296.
15. Cutler DJ, Haraura M, Reed HE, et al. (2003) The mouse VPAC2 receptor confers suprachiasmatic nuclei cellular rhythmicity and responsiveness to vasoactive intestinal polypeptide *in vitro*. *Eur J Neurosci* 17:197– 204.
16. Brown TM, Colwell CS, Waschek JA, Piggins HD (2007) Disrupted neuronal activity rhythms in the suprachiasmatic nuclei of vasoactive intestinal polypeptide-deficient mice. *J Neurophysiol* 97:2553–2558.
17. Aton SJ, Colwell CS, Harmar AJ, Waschek J, Herzog ED (2005) Vasoactive intestinal polypeptide mediates circadian rhythmicity and synchrony in mammalian clock neurons. *Nat Neurosci* 8:476–483.
18. Ciarleglio CM, Gamble KL, Axley JC, et al. (2009) Population encoding by circadian clock neurons organizes circadian behavior. *J Neurosci* 29:1670–1676.
19. Harmar AJ, Marston HM, Shen S, et al. (2002) The VPAC(2) receptor is essential for circadian function in the mouse suprachiasmatic nuclei. *Cell* 109:497–508.
20. Colwell CS, Michel S, Itri J, et al. (2003) Disrupted circadian rhythms in VIP- and PHI-deficient mice. *Am J Physiol* 285:R939–R949.
21. Paxinos G, Franklin KBJ (2008) The Mouse Brain in Stereotaxic Coordinates. Academic Press, Waltham, MA
22. Eilers P (2003) A perfect smoother. *Anal Chem* 75:3631–3636.
23. Houben T, Deboer T, Oosterhout F, Meijer JH (2009) Correlation with behavioral activity and rest implies circadian regulation by SCN neuronal activity levels. *J Biol Rhythms* 24:477–487.
24. Sheward WJ, Naylor E, Knowles-Barley S, et al. (2010) Circadian control of mouse heart rate and blood pressure by the suprachiasmatic nuclei: behavioral effects are more significant than direct outputs. *PLoS ONE* 5:e9783.
25. Hannibal J, Hsiung HM, Fahrenkrug J (2011) Temporal phasing of locomotor activity, heart rate rhythmicity, and core body temperature is disrupted in VIP receptor 2-deficient mice. *Am J Physiol Regul Integr Comp Physiol* 300:R519–R530.
26. Schroeder A, Loh DH, Jordan MC, Roos KP, Colwell CS (2011) Circadian regulation of cardiovascular function: a role for vasoactive intestinal peptide. *Am J Physiol Heart Circ Physiol* 300:H241–H250.

27. Bechtold DA, Brown TM, Luckman SM, Piggins HD (2008) Metabolic rhythm abnormalities in mice lacking VIP-VPAC2 signaling. *Am J Physiol Regul Integr Comp Physiol* 294:R344–R351.
28. Hu WP, Li JD, Colwell CS, Zhou QY (2011) Decreased REM sleep and altered circadian sleep regulation in mice lacking vasoactive intestinal polypeptide. *Sleep* 34:49–56.
29. Loh DH, Abad C, Colwell CS, Waschek JA (2008) Vasoactive intestinal peptide is critical for circadian regulation of glucocorticoids. *Neuroendocrinology* 88:246–255.
30. Buijs RM, Scheer FA, Kreier F, et al.(2006) Organization of circadian functions: interactions with the body. *Prog Brain Res* 153:341–360.
31. Antle MC, Silver R (2005) Orchestrating time: arrangements of the brain circadian clock. *Trends Neurosci* 28:145–151.
32. Kalsbeek A, Palm IF, La Fleur SE, et al. (2006) SCN outputs and the hypothalamic balance of life. *J Biol Rhythms* 21:458–469.
33. Vosko AM, Schroeder A, Loh DH, Colwell CS (2007) Vasoactive intestinal peptide and the mammalian circadian system. *Gen Comp Endocrinol* 152:165–175.
34. Welsh DK, Takahashi JS, Kay SA (2010) Suprachiasmatic nucleus: cell autonomy and network properties. *Annu Rev Physiol* 72:551–577.
35. Loh DH, Dragich JM, Kudo T, et al. (2011) Effects of vasoactive intestinal peptide genotype on circadian gene expression in the suprachiasmatic nucleus and peripheral organs. *J Biol Rhythms* 26:200–209.
36. Maywood ES, Reddy AB, Wong GKY, et al. (2006) Synchronization and maintenance of timekeeping in suprachiasmatic circadian clock cells by neuropeptidergic signalling. *Curr Biol* 16:599–605.
37. Hughes AT, Guilding C, Piggins HD (2011) Neuropeptide signaling differentially affects phase maintenance and rhythm generation in SCN and extra-SCN circadian oscillators. *PLoS ONE* 6:e18926.
38. Maywood ES, Chesham JE, O' Brien JA, Hastings MH (2011) A diversity of paracrine signals sustains molecular circadian cycling in suprachiasmatic nucleus circuits. *Proc Natl Acad Sci USA* 108:14306–14311.
39. Meijer JH, Watanabe K, Détàri L, Schaap J (1996) Circadian rhythm in light response in suprachiasmatic nucleus neurons of freely moving rats. *Brain Res* 741:352–355.
40. Meijer JH, Watanabe K, Schaap J, Albus H, Détári L (1998) Light responsiveness of the suprachiasmatic nucleus: long-term multiunit and single-unit recordings in freely moving rats. *J Neurosci* 18:9078–9087.
41. Panda S (2007) Multiple photopigments entrain the mammalian circadian oscillator. *Neuron* 53:619–621.
42. Ecker JL, Dumitres ON, Wong KY, et al. (2010) Melanopsin-expressing retinal ganglion-cell photoreceptors: cellular diversity and role in pattern vision. *Neuron* 67:49–60.
43. Lall GS, Revell VL, Momiji H, et al. (2010) Distinct contributions of rod, cone and melanopsin photoreceptors to encoding irradiance. *Neuron* 66:417–428.
44. Berson DM, Dunn FA, Takao M (2002) Phototransduction by retinal ganglion cells that set the circadian clock. *Science* 295:1070–1073.
45. Hannibal J (2002) Pituitary adenylate cyclase-activating peptide in the rat central nervous system: an immunohistochemical and in situ hybridization study. *J Comp Neurol* 453:389–417.
46. Deboer T, Vansteensel MJ, Détàri L, Meijer JH (2003) Sleep states alter activity of suprachiasmatic nucleus neurons. *Nat Neurosci* 6:1086–1090.
47. Vansteensel MJ, Yamazaki S, Albus H, et al. (2003) Dissociation between circadian Per1 and neuronal and behavioral rhythms following a shifted environmental cycle. *Curr Biol* 13:1538–1542.
48. Power A, Hughes ATL, Samuels RE, Piggins HD (2010) Rhythmpromoting actions of exercise in mice with deficient neuropeptide signalling. *J Biol Rhythms* 25:235–246.
49. Meijer JH, Schaap J, Watanabe K, Albus H (1997) Multiunit activity recordings in the suprachiasmatic nuclei: *in vivo* versus *in vitro* models. *Brain Res* 753:322–327.
50. Yamazaki S, Kerbeshian MC, Hocker CG, Block GD, Menaker M (1998) Rhythmic properties of the hamster suprachiasmatic nucleus *in vivo*. *J Neurosci* 18:10709–10723.
51. Schaap J, Meijer JH (2001) Opposing effects of behavioral activity and light on neurons of the suprachiasmatic nucleus. *Eur J Neurosci* 13:1955– 1962.
52. Nakamura TJ, Nakamura W, Yamazaki S, et al. (2011) Age-related decline in circadian output. *J Neurosci* 31:10201–10205.
54. Beersma DG, van Bunnik BA, Hut RA, Daan S (2008) Emergence of circadian and photoperiodic system level properties from interactions among pacemaker cells. *J Biol Rhythms* 23:362–373.

55. Refenetti R (2002) Compression and expansion of circadian rhythm in mice under long and short photoperiods. *Integr Physiol Behav Sci* 37:114– 127.
56. Hazlerigg DG, Ebling FJ, Johnston JD (2005) Photoperiod differentially regulates gene expression rhythms in the rostral and caudal SCN. *Curr Biol* 15:R449–R450.
57. Inagaki N, Honma S, Ono D, Tanahashi Y, Honma K (2007) Separate oscillating cell groups in mouse SCN couple photoperiodically to the onset and end of daily activity. *Proc Natl Acad Sci USA* 104:7664–7669.
58. Naito E, Watanabe T, Tei H, Yoshimura T, Ebihara S (2008) Reorganization of the suprachiasmatic nucleus coding for day length. *J Biol Rhythms* 23:140–149.
59. Sosniyenko S, Hut RA, Daan S, Sumova A (2009) Influence of photoperiod duration and light–dark transitions on entrainment of Per1 and Per2 gene and protein expression in subdivisions of the mouse SCN. *Eur J Neurosci* 30:1802–1814.
60. Liu AC, Welsh DK, Ko CH, et al. (2007) Intercellular coupling confers robustness against mutations in the SCN circadian clock network. *Cell* 129:605–616.